Title
Review of CERN Heavy-Ion Physics

Author
Odyniec, G.J.

Publication Date
1991-11-01

Lawrence Berkeley Laboratory
UNIVERSITY OF CALIFORNIA

Invited paper presented at the 2nd International Workshop on Relativistic Aspects of Nuclear Physics, Rio de Janeiro, Brazil, August 28–30, 1991, and to be published in the Proceedings

Review of CERN Heavy-Ion Physics

G. Odyniec

November 1991

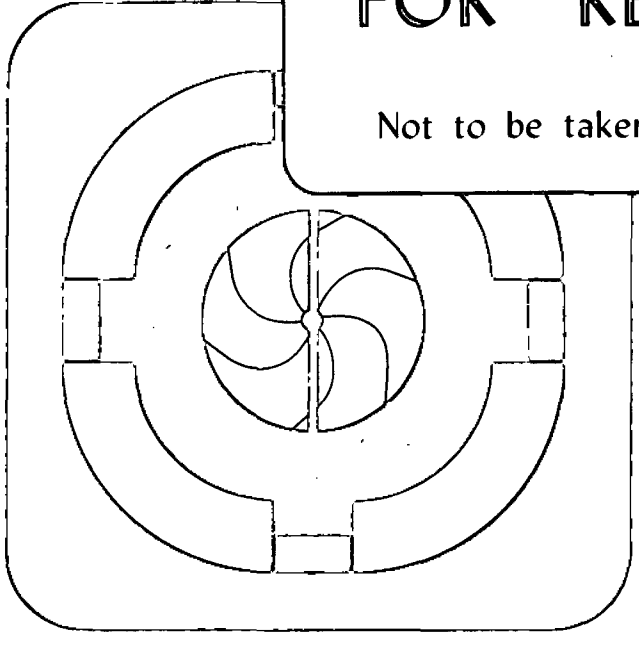

Prepared for the U.S. Department of Energy under Contract Number DE-AC03-76SF00098

DISCLAIMER

LBL-31483

Submitted to World Scientific Publishing Co.

Review of CERN Heavy-Ion Physics

Invited paper presented to the 2nd International Workshop on
Relativistic Aspects of Nuclear Physics,
Rio de Janeiro, Brazil, August 28-30, 1991

Grazyna Odyniec
Nuclear Science Division, Lawrence Berkeley Laboratory
University of California, Berkeley, CA 94720

November 1991

This work was supported by the Director, Office of Energy Research, Division of Nuclear Physics of the Office of High Energy and Nuclear Physics of the U.S. Department of Energy under Contract DE-AC03-76SF00098

Review of CERN Heavy-Ion Physics

Grazyna Odyniec
Nuclear Science Division
Lawrence Berkeley Laboratory
1 Cyclotron Road
Berkeley, CA 94720

Abstract: Results from the heavy-ion experiments at the CERN SPS are reviewed in the context of possible formation and identification of a quark-gluon plasma (QGP).

1. INTRODUCTION

The ultimate goal of studying nucleus-nucleus collisions at very high energies is the quest for quark-gluon plasma (QGP). Quantum chromodynamics predicts unambiguously [1] that above a critical temperature of about 200 MeV, nuclear matter, or even the vacuum itself, if excited to a sufficiently high energy density (of about few GeV/fm^3) over an extended region will undergo a phase transition into a new state of matter in which quarks and gluons are no longer confined inside individual nucleons and mesons, but are free to wander over distances much longer than 1 fermi, the characteristic size of a hadron.

Cosmologists believe that such a state of nuclear matter is not new at all, because the entire universe existed as a quark-gluon plasma during the first 10 microseconds of the Big Bang.

In the laboratory environment, similar extreme conditions could be created in nucleus-nucleus reactions by converting the initial relative c.m. energy into internal excitation of a "fireball" formed at rapidities intermediate between those of target and projectile, if provided with sufficient beam energy and adequate stopping power.

Head-on heavy-ion collisions, which generate the highest energy density in a large interaction volume, are the most favorable candidates for QGP searches. In the ideal case one would study central collisions of symmetric systems where there will be no cold nuclear matter (spectators) to complicate the interpretation of the experimental results.

The QCD prediction is quite firm that a quark-gluon plasma exist at sufficiently high energy density, but the theory have yet to say unambiguously whether the quark-gluon plasma is separated from ordinary nuclear matter by a first- or second-order thermodynamic phase transition, or by something much more gradual. Therefore the experimenters are looking simultaneously for signatures of existing plasma and for signatures of phase transition. Other complications arise from the fact that quark-gluon plasma can be formed, if at all, only in the early stages just after collision; when the secondary particles produced in the interaction reach the detectors, any deconfined system will have passed through the quark-hadron phase transition. So the experimenters are left with the additional task of finding a signatures of something that existed prior to any measurements and was probably distorted during the space-time evolution of the collision.

Several candidate signatures for the formation of a quark-gluon plasma have been proposed. Observations on:

- increased strange particle abundance due to high $\bar{s}s$ quark density [2],
- quenching of quarkonium production [3]

and

- increased production of "thermal" direct photons and leptons [5]

provide information on plasma phase. One can learn about expansion, cooling and hadronization from:

- the characteristic plateau in $<p_t>$ as a function energy density [6, 41],
- a long hadronization time and a large freezout volume due to the high density of produced particles [7],
- fluctuations during hadronization leading to particle clustering in rapidity ("intermittency") [7,52],
- strange matter ("strangelets") [8].

Finally, a few words of caution:

Qualitatively similar phenomena are also expected in dense hadronic matter due to rescattering. Therefore, only a systematic comparison of p-p, p-A and A-A' collisions may allow the separation of genuine high-matter-density effects from phenomena characteristic for convolution of p-p interactions. For the same reason, simultaneous observation of more than one of the QGP signatures is essential.

In this review, the current status of the selected experimental results that are relevant to equilibration and QGP formation in nucleus-nucleus collisions, is presented.

2. CERN EXPERIMENTS

An exploratory program to investigate the properties of the nucleus-nucleus collisions at high energy was begun at CERN in 1986 with ^{16}O beams at 60 GeV/N and 200 GeV/N. During the second heavy ion run, in 1987, ^{32}S beams were accelerated to 200 GeV/N. After the initial pilot runs of two weeks each, the long term heavy-ion program was established at CERN SPS.

Almost all CERN data was taken at 200 GeV/N. Given the substantial degree of stopping reported at BNL energies [20] (earlier publications [9] reported even full stopping, which was later recognized as primarily an effect of limited acceptance in phase space), one expects significant degree of nuclear transparency at such a high energy (the energy in the c.m.s. at 200 GeV/N is 4 times higher than at BNL) which might complicate interpretation of the experimental results.

Another complication caused by the high energy is related to detection limitations. The rapidity window at CERN is 6, (as compared with only 3.4 at BNL), which in principle, should give less overlap between the target, projectile, and interaction rapidity regions. In practice, however particles of rapidity 3 in laboratory system (central rapidity for symmetric systems at CERN) are too fast to be identified in existing detectors. Consequently, experiments at 200 GeV/N cannot identify particles in the most interesting region, where there is the highest probability of finding traces of the hypothetical plasma phase. The situation looks much more favorable at 60 GeV/N, but almost no data has been taken there.

Table 1 lists CERN experiments, which have been taking data during heavy-ion runs, their main detectors and observables.

Table 1.

Experiment	Main Detector	Main Observables
NA 34	Magn.spect.+Calo.+TOF	low-mass dimuons,K,π
NA 35	Stream.cham.+TPC+Calo.	Λ, $\bar{\Lambda}$, K^o,K^+,K^-,"p",π
NA 36	TPC+Calo.	Λ, $\bar{\Lambda}$, K^o, (Ξ^-, $\bar{\Xi}^-$)π
NA 38	Dimuon spect.	high-mass dimuons Φ,J/ψ
WA 80	Plastic ball+calo.	π^o, γ, target fragments
WA 85	Ω-spect.+MWPC+μ-Si.	Λ, $\bar{\Lambda}$, Ξ^-, $\bar{\Xi}^-$

As shown in Table 1 - there are two categories of experiments: spectrometer experiments (NA34, NA38, WA85) and chamber experiments (NA35, NA36). Two types of nuclear reactions were studied: symmetric (^{32}S-S) and asymmetric (^{16}O, ^{32}S on diverse targets) ones. The particular advantage of the symmetric system, e.g. ^{32}S-S (NA35), both in mass and isospin is that the measurements of particles in one hemisphere of the c.m.s. provides complete information on all produced particles in full phase space. The disadvantage is, no doubt, the presence of significant transparency at such a light system at 200 GeV/N. In asymmetric reactions, i.e. the ^{32}S-W collisions (WA85) or ^{32}S-Pb (NA36), there is the advantage of much greater baryon-number stopping. There are difficulties, however, in interpreting the data, which are associated with the overlap of the various kinematic regions and with the presence of the cold nuclear matter.

3. GLOBAL CHARACTERISTICS OF THE COLLISION

Information on the geometry of nucleus-nucleus interactions is essential for understanding and interpretation of the experimental data. Glancing collisions (large impact parameter b) are of little interest (except for some conventional nuclear physics studies or as a reference). The main emphasis is, of course, on head-on collisions (small b) which generate the highest energy densities. A simple "multiplicity" trigger, looking for events which produce far more particles than the average, can provide a fast first cut at identifying events that might be of interest. Fig.1 shows charge multiplicity distribution obtained with the NA36 TPC in ^{32}S-Pb interactions at 200 GeV/N. The shape of the cross section reflects the geometry of an (asymmetric) collision: the large cross section at low multiplicity corresponds to peripheral events (large b), rather long and flat plateau encountered for decreasing impact parameter (and increasing number of participants) followed by a

dramatic break (central collisions, b=0) and a steep decline (with fluctuation in the tail). Due to the linear relation between charge-particle multiplicity and transverse energy, the dN/dE_t spectrum reflects the same features. Equivalent information can be also obtained from measurements of rapidity or of longitudinal energy in the event. Plotting longitudinal vs transverse energy in an event particularly facilitates determination of the nucleus-nucleus collision geometry. Fig.2 shows an anti-correlation between the transverse energy and the energy remaining in the projectile and target fragmentation regions observed in experiment NA35 at ^{32}S-Au reactions at 200 GeV/N.

4. DYNAMICS OF THE COLLISION

4.1 Energy Density and Stopping Power

Transition to the hypothetical quark-gluon plasma phase might only take place when the energy density and temperature reached in the early stages of the collision exceed the critical values predicted by QCD [1]. Creation of a high energy density requires large energy deposition from the longitudinal motion of the projectile into interaction volume. The degree to which an incident particle transforms its longitudinal energy into excitation and transverse degree of freedom is called stopping power. Rapidity distributions and transverse energy spectra of produced and primordial particles are studied for information on stopping power, degree of thermalization, and energy density.

Fig.3 shows the rapidity distribution of negative hadrons in central ^{32}S-S collisions at 200 GeV/N (NA35). The peak position is consistent with a simple geometrical overlap picture of the collision. The solid line represents the spectrum of thermally produced pions expected from a source at a temperature of 160 MeV. The experimental distribution is Gaussian in shape and is broader than would be expected from emission of an isotropic fireball [10]. The same behavior was observed for K^o's and Λ's [11]. Clearly the incoming longitudinal energy is not completely thermalized, and some fraction of the longitudinal motion is still present in the produced particles.

There have been a number of attempts to describe the rapidity spectrum of produced particles at CERN energies with string-type models (Fritiof/Lund) and with Landau hydrodynamical models. Both of approaches were reasonably successful in predicting the measured distributions. However one must be careful when comparing with models based on superposition of p-p (which ignore "trivial" final state interactions!) because to little is presently known about strings and their properties. In particular, it is not clear what happens when strings overlap in space. At CERN energies the estimated string density is approximately few/fm^2.

Much less information is available concerning the primordial protons present in incident nuclei, which could provide the most direct information on stopping power and the baryon density. CERN experiments do not have

capability of identifying protons in nucleus-nucleus collisions with the present apparatus. Instead, experiment NA35 has determined the rapidity distribution of "charge flow" [12] in isospin-symmetric ^{32}S-S reaction at 200 GeV/N from the difference between the positive and negative particle distributions. Fig.4 shows the rapidity distribution of "protons" obtained in this way for central and peripheral ^{32}S-S collisions at 200 GeV/N. The data points are determined in the backward hemisphere (solid circles) and reflected at y=3 (open circles). Considering the light system, the spectrum is remarkably flat and indeed exhibits considerably more stopping than predicted by the Fritiof/Lund model. Rescattering which was included in some versions of Venus2 [13] and the RQMD [14] models, leads to an increased rapidity loss and could describe the high baryon densities observed even at midrapidity.

The assumption of a baryon-free region is certainly no longer justified at the present energies and must await future machines.

The E_t distribution over a large part of the phase space was measured in the early stage of the CERN heavy ion programme by several collaborations [15,16,17]. In order to relate stopping power to measured transverse energy, the ratio of E_t/E_{tmax} is calculated. Here E_t is the measured transverse energy in the experimental acceptance extrapolated to full phase space, and E_{tmax} is the maximum transverse energy emitted in 4π solid angle by an isotropic source located in the center-of-mass of the participants. At 60 GeV/N stopping for oxygen projectile, as calculated using the E_t/E_{tmax} ratio ranges from 0.7 on light targets to 0.9 on heavy targets. At 200 GeV/N - for oxygen and sulphur beams the same quantity ranges from 0.4 to 0.7.

The energy density produced in the collision might be estimated from the "tails" of transverse energy distributions using Bjorken kinematics [18], where the energy density in the interaction region at time t after the collision is given by the formula:

$$\varepsilon = \frac{1}{\pi(r_o \times A^{1/3})^2} \times \frac{1}{t} \times \frac{dE_t}{dy}$$

The energy is taken as the transverse energy dE_t within a rapidity interval dy. The first term in the expression is the cross sectional area of the interaction zone. The term tdy is the length of the element dy at time t after the collision. The quantity dE_t/dy is measured by calorimetry. Fig.5 shows a transverse energy spectra obtained for the ^{16}O-Au system at 60 GeV/N and at 200 GeV/N and for ^{32}S-Au at 200 GeV/N (NA35). The shape of the distributions is the same, of course, as the one presented on Fig.1 due to linear dependence between multiplicity and E_t. The shoulders at 50 GeV for ^{16}O-Au (60GeV/N), 90 GeV for ^{16}O-Au (200 GeV/N) and 150 GeV for ^{32}S-Au (200 GeV/N) correspond to central collisions in which all the nucleons in the projectile interact with the target. For such collisions, the energy density as

estimated within the experimental acceptance and assuming 1 fm/c for the t value amounts to ~1.5 GeV/fm^3 for ^{16}O-Au at 60 GeV/N, ~2.5 GeV/fm^3 for ^{16}O-Au at 200 GeV/N and ~3 GeV/fm^3 for ^{32}S-Au at 200 GeV/N.

Therefore, one may conclude that there is an a priori case that the energy density of ~2-3 GeV/fm^3 which is estimated to be necessary for quark-gluon plasma formation may have been reached. However, this estimate of ε_o is very imprecise for two reasons. One is that the choice of t=1 fm/c is somewhat arbitrary. It is chosen to correspond to the hadronization time τ_o, the time required to form a hadron. This quantity is not well understood. The other source of imprecision is that the formula is derived under assumptions appropriate to infinite energies. In particular, the formation time of the hot system is assumed to be zero, and the system after formation is assumed to be thin disk. This is at variance with the actual situation in which the transition time for e.g. an ^{16}O projectile at 200 GeV/N to pass through a Au nucleus is approximately 2 fm/c.

4.2 Temperature

The next question is whether sufficient temperature is reached in the interaction volume to create a quark-gluon plasma. Using relativistic thermodynamics, developed by Hagedorn [19], for a single isotropic fireball at temperature T, a Boltzman distribution of momenta of emitted particles integrated over rapidity leads to the transverse mass distribution given by formula:

$$\frac{dn}{dm_t} = \text{const} \times m_t^{3/2} \times \exp(-m_t/T)$$

for large m_t/T, where $m_t = \sqrt{p_t^2 + m^2}$. Therefore, one needs to examine whether $m_t^{-3/2} dn/dm_t$ is an exponentially decaying function of m_t/T at large m_t.

Figs. 6 and 7 show plots of this type for π's, K's, protons and Λ's measured by NA35 collaboration in 200 GeV/N ^{16}O-Au and ^{32}S-S collisions. The extracted inverse slopes are in the range 180-200 MeV. The fits are linear, with the exception of the soft pions and are very nearly parallel. For ^{32}S-S the m_t spectrum is somewhat flatter than that of the other particles. Similar results were reported by NA34 collaboration for the reaction ^{32}S-W at 200 GeV/N.

Roughly speaking, the pion spectra observed in nuclear collisions at CERN can be described by 2 components (~50 and ~200 MeV) while all secondaries by only one (~200 MeV). This is not the case at lower energies (AGS) or at larger ones (Tevatron) where heavier secondaries have larger T.

At the simplest level, m_t scaling should hold in purely thermal models, reflecting the temperature at which particles are radiated. The measured

temperature of about ~200 MeV (Fig.6,7) is remarkably close to that theoretically predicted for formation of quark-gluon plasma. However, the interpretation of the spectra in terms of a thermal distribution is an oversimplification due to complicating factors. These include the decay of resonances, expansion and cooling prior to particle emission and hydrodynamic flow, which were not taken to the account. It is only at high transverse momenta that the effects of initial temperature may survive, as suggested by data.

5. EXPERIMENTAL RESULTS ON SPECIFIC QGP SIGNATURES

The conclusion of the previous sections, that the initial conditions reached in the collisions are suitable for production of a quark-gluon plasma, is not a surprise: this was the initial motivation for designing apparatus and carrying out the studies. However, observation of signatures of the plasma phase would be a surprise, since the size of the interaction volume for light projectiles like ^{16}O(~50fm) or ^{32}S(~90 fm) is expected to be too small for equilibrium to be establish.

To the great satisfaction of all physicist, the CERN heavy ion program has encountered quite a few surprises. However, various post hoc explanations have been proposed in order to avoid the necessity of conclusions implying either a phase transition or plasma formation. In this chapter, experimental results on specific QGP signatures are reviewed and their interpretations are discussed.

5.1 Pion Interferometry

All observed particles are measured only in momentum space. Therefore any information on source size is a result of theoretical interpretation of the spectra. Relatively direct and model independent way of studying the space-time dimensions of source of emitting particles is intensity interferometry, originally developed by Hanbury-Brown and Twiss (HBT) in 1950 to determine the radii of visual stars [27]. In brief, the method is based on the assumption that particles (bosons: in astrophysics-photons, here-pions) are described by plane waves. Antisymmetrization of their wave functions leads to correlation in momentum-energy space, which is related via a Fourier transformation to the source distribution in space-time. Interpretation of measured correlation functions is complicated by the effects like Coulomb repulsion, Lorentz-frame dependence, the non-static character of the source, resonance decays, limited acceptance etc. An in-depth presentation of measurements of HBT correlations in relativistic heavy ion collisions appears elsewhere in the Proceedings of this Workshop [30].

Here are summarized the main results.

The NA35 Collaboration has measured the correlation function with negative pions in a number of reactions [21,22,23]. In ^{16}O-Au at 200 GeV/N, near midrapidity, a source radius of 8.1±1.6 fm was observed, with a chaoticity parameter $\lambda = 0.77 \pm 0.19$ which measures the strength of the correlation at zero 4-momentum difference ($\lambda = 1$ for completely chaotic emission). Away from mid-rapidity a smaller source radius ~4 fm was observed, with a chaoticity parameter λ ~0.3. The radius observed away from mid-rapidity is roughly consistent with the size of the projectile nucleus, though the λ parameter value is not explained. Similar (preliminary) results were obtained in ^{32}S-Au and ^{32}S-Ag, both at 200 GeV/N. Those results are based on the limited statistics (see ref.[30] for discussion), and confirmation with better statistics is needed.

A quantitative explanation of the surprisingly large radius, assuming that the freeze-out volume depends on the particle density, was proposed in [24]. Fig.8 shows dependence of freeze-out radii (R_f) on charge particle density $\sqrt{\frac{dN^{\pm}}{dy}}$ in hadron-hadron and nucleus-nucleus collisions. The line represents fit to the data:

$R_f = 0.84\sqrt{\frac{dN^{\pm}}{dy}}$ [24].

The large source radius does not provide direct evidence of quark-gluon plasma formation. If however the radius of 8 fm is a freeze-out radius as interpreted above, it means that at radii of 4 fm, corresponding to the presumed initial volume of the interaction region, the particles in the system cannot be pions [25]. It is just not possible to fit them all in. Whether the initial system is better described in terms of a hadronic gas or as a quark-gluon plasma is an open question. In the end it may turn out to be primarily a matter of simplicity and economy of parameters, in which case a description in terms of quarks and gluons will have an advantage.

5.2 Strangeness Production

The production of strange particles is expected to be enhanced by the quark-gluon plasma as compared with a thermalized hadronic gas, as has been originally proposed by Rafelski [28]. A recent review with detailed calculations can be found in [29]. The main arguments are:

- a lower energy threshold in plasma,
- increased strangeness density,
- higher production rates due to a shorter time constant,
- enhanced production of antistrange baryons as a consequence of a large ratio of $\bar{s}$ to $\bar{u}$ and $\bar{d}$ quarks in the baryon rich region,
- and, perhaps most important, the presence of a large number of gluons in the plasma state.

Furthermore, the information carried by the strange particles is expected to be preserved in the evolution of the hadronic matter following the dissociation of the QGP [28,29].

Although it is clear that states of very high energy density and high temperatures are formed already in relativistic heavy-ion collisions at CERN energies, it has not been shown experimentally that equilibrium (either thermal or chemical) has been reached. Note that the strangeness abundance depends strongly on the degree of equilibrium achieved, either by a plasma or a hadronic gas.

At CERN five experiments have collected data on strangeness production: NA34, NA35, NA36, NA38 and WA85.

The NA34 Spectrometer covers only the target fragmentation region ($0.8<y<1.3$) where scattering on cold nuclear matter is dominant. Therefore the results [26] are not of direct relevance to the issue of the QGP.

The NA35 experiment studied 60 and 200 GeV/N p and ^{16}O beams and 200 GeV/N ^{32}S beams incident on nuclear targets varying in mass from S to Au. In ^{16}O-Au and p-Au reactions at 60 and 200 GeV/N, investigation of the quark-gluon plasma production is hampered by inadequate predictions of production via hadronic processes. Extraction of model-independent quantities such as particle yield ratios is very difficult because the experimental acceptances in (p_t, y) are neither complete nor identical for various particles. Results on ^{16}O-Au and p-Au will not be discussed here since they are not directly related (acceptance covers backward of mid-rapidity region of phase space only) to the issues of QGP formation. However, particle yields and spectra in the limited acceptance, as well as detailed information on the procedure, can be found in [11]. The situation looks different in ^{32}S-S collisions. Figs. 9 A, B and C show the ratios of the average number of Λ, $\bar{\Lambda}$ and K^o to the total number of observed negative particles (mainly pions) in ^{32}S-S collisions at 200 GeV/N as a function of the event multiplicity. The three points plotted in each figure represent peripheral, intermediate, and central collisions respectively. The Λ/π, $\bar{\Lambda}/\pi$ and K^o/π ratios increase linearly with multiplicity and reach 2-3 times the value expected from nucleon-nucleon collisions (dashed lines on Figs.9A, B and C represent Fritiof calculations). Note that other features of the same collisions are in very good agreement with Fritiof predictions [31]. Furthermore, the y-distribution (Fig. 10A) in ^{32}S-S collisions is flat in the interval $1.5<y<4.5$. In particular, it is non zero in the central rapidity region which is believed to be almost baryon-free, since the numbers of positive and negative particles (mainly pions) are nearly equal. Therefore, one would expect few if any Λ's there, unless " ... a QGP fireball had been formed ... "[29]. The next very important question is, where did the $\bar{\Lambda}$'s whose ratio grows with the event multiplicity as fast as in the Λ and K^o cases, come from? Fig. 10B shows the rapidity distribution of $\bar{\Lambda}$'s, with the maximum observed in the central rapidity region. So, Λ's and $\bar{\Lambda}$'s are produced "together" (i.e. in the same rapidity region), making the argument

in favor of QGP formation much stronger. Table 2 gives a comparison of negative and strange particle production per event in 4π acceptance in p-p and ^{32}S-S collisions at 200 GeV/N.

Table 2.

$<h^->$	2.85	$\pm$	0.04	~36x ------>	103 ± 5
$<\bar{\Lambda}>$	0.013	$\pm$	0.004	~115x! ------>	1.5 ± 0.4
$<\Lambda>$	0.095	$\pm$	0.01	~86x ------>	8.2 ± 0.9
$<K^o>$	0.17	$\pm$	0.01	~62x ------>	10.7 ± 2

One sees that the yield of $\bar{\Lambda}$'s in ^{32}S-S is 1.5 per event (!), 115 times greater than in p-p collisions. This enhancement should be compared with the 36-fold enhancement of the negatively charged tracks.

This strangeness enhancement is the most striking result from the current experiments investigating possible QGP formation. No explanation for such an enhancement has been provided by any type of cascading in a hadronic gas. There is no imaginable process that could produce such a number of $\bar{s}$ quarks within a hadronic fireball scenario.

The main detector of the NA35 experiment, the large-volume streamer chamber, can accumulate and measure data samples of the order of few hundred events. NA36, with its TPC, is capable of analyzing strange particle production with the statistics an order of magnitude higher [32]. Fig.11 shows invariant mass plots from NA36 for Λ's, $\bar{\Lambda}$'s and K^o's with magnificent statistics. Analysis is in progress and results are to be expected soon.

There are ambiguities in interpreting the total strangeness content in QGP and HG models which are related to our present ignorance of the reaction dynamics. Therefore, the strangeness density, which is undoubtedly higher in a QGP than in a HG [33,34] has become the experimental observable of primary interest. This quantity is indirectly accessible to measurement through the observation of multistrange baryon abundances, i.e., cascades and omegas.

For the first time, production of Ξ and $\bar{\Xi}^-$ has been observed by the WA85 experiment in ^{32}S-W and p-W interactions at 200 GeV/N. The omega magnetic spectrometer used by WA85 is optimized to measure strange baryons in the acceptance region $2.3 < y < 3.0$ and $p_t > 1$ GeV/c. The following results were obtained in ^{32}S-W (200 GeV/N) collisions: $\bar{\Xi}^-/\Xi = 0.39 \pm 0.07$, $\bar{\Xi}^-/\bar{\Lambda} = 0.60 \pm 0.20$, $\bar{\Lambda}/\Lambda = 0.13 \pm 0.03$, $\Xi/\Lambda = 0.20 \pm 0.04$ [55]. The Λ sample includes Λ's from Σ^o, whereas the contamination arising from cascade decays has been corrected for. For comparison in p-W $\bar{\Xi}^-/\Xi = 0.027 \pm 0.06$. The

production of both Λ's and $\bar{\Lambda}$'s increases by ~70% when going from p-W to ^{32}S-W, while the $\bar{\Lambda}/\Lambda$ ratio is essentially constant.

This is comparable to the value of ~77% from NA35 [35] for system ^{16}O-Au and p-Au, calculated in NA35 acceptance scaled down to match WA85 coverage. The $\bar{\Xi}^-/\ \bar{\Lambda}$ ratio observed here is about five times greater than that measured at ISR (although both are having large errors).

It appears that this strong overall increase in antibaryon production will be difficult to explain using non-QGP models.

The NA38 dimuon spectrometer measured mass and p_t spectra of dimuons produced in the 200 GeV/N p-U, ^{16}O-U, and ^{32}S-U reactions [36]. To reduce combinatorial background from kaon- and pion-decays in the μ-pair spectrum, p_t and p_L cuts were imposed, which reduced the available phase space to $p_t^{\mu\mu} > 1.3$ GeV/c and $2.8 < y < 4$. The measured $\mu^+\mu^-$ mass spectra (Fig.12) for p-U, ^{16}O-U, and ^{32}S-U at 200 GeV/N show evidence for Φ,ρ and ω vector mesons [37]. The clear double-peak structure, as seen in the muon-pair mass region of 0.6-1.2 GeV, becomes more pronounced with increasing mass of the colliding system. By fitting $\mu^+\mu^-$ mass spectra (solid lines on Fig.12) under the assumption of an equal-production cross section for ω and ρ, a $\Phi/(\omega+\rho)$ ratio is extracted and reaches the very high value of 0.59 ± 0.02 in ^{32}S-U collisions. The ratio $\Phi/(\omega+\rho)$ versus $E_t\, A^{-2/3}$ in ^{16}O-U and ^{32}S-U collisions, as normalized to the result for average p-U reactions, is shown in Fig. 13. One observes that it rises with energy density (which is ~$E_t\, A^{-2/3}$)to 3 times the p-U value and scales also with the energy density.

This new observation parallels that of the NA35 Collaboration using ^{32}S-S collisions, where an enhancement of the ratios of kaons, Λ's and $\bar{\Lambda}$'s over the total multiplicity as a function of centrality of the collision was seen. Both findings point to enhanced strangeness production in central A-A collisions.

An enhancement of the hidden-strangeness Φ-meson production in nucleus-nucleus collisions compared with its value in p-p was previously predicted [38] as a possible signal for QGP formation.

However, hadronic-gas models are also able to describe Φ-meson enhancement satisfactorily. A qualitative description of the trend of the data was obtained [39] by solving the rate equations for Φ-production and Φ-absorption via secondary collisions in the dense reaction zone (the solid line in Fig.13). Another explanation, based on the substantial increase of Φ production cross section due to the $K + K \rightarrow \Phi + \rho$ and $K + \Lambda \rightarrow \Phi + N$ processes was also successful in fitting the data [40].

5.3 $\langle p_t \rangle$ As A Function of Energy Density

In heavy ions collisions, the dependence of the transverse momenta of hadrons on multiplicity (or E_t) translates into the dependence of the temperature of the (thermalized) system on the energy density.

In the pure hadronic gas, temperature is expected to rise linearly with energy density. During a phase transition, one would expect an initial rise, then a plateau at the region of phase coexistence, followed by a second rise due to the onset of the pure quark phase. Such a behavior was expected to be one of the experimentally "easiest" signatures for QGP formation [41].

To analyze experimental data one needs to assume that $\langle p_t \rangle$ of pions reflects temperature of the system, and that the increasing charge multiplicity or E_t produced in the collision is proportional to the increasing energy density. Fig.14 shows the distributions of $\langle p_t \rangle$ for π's, K's, antiprotons and lambdas (preliminary) vs charged particle multiplicity for p-$\bar{p}$ collisions at the Tevatron ($\sqrt{S}$ = 1.8 TeV) [42]. The calculation of $\langle p_t \rangle$ was made for particles with p_t<1.5 GeV/c, so the value should not be influenced by hard scattering. For pions and kaons no second rise was observed, whereas for protons and lambdas the $\langle p_t \rangle$ distributions are clearly rising into the second slope.

Such a behavior was not observed at CERN experiments. Fig. 15 shows the dependence of $\langle p_t \rangle$ on charged particle multiplicity for heavy ion collisions measured by WA80 collaboration at 60 and 200 GeV/N. An initial rise of $\langle p_t \rangle$ follow by a flattering is observed; there is no indication of the second slope.

5.4 J/ψ Suppression

Suppression of the J/ψ signal relative to the Drell-Yan continuum was regarded as one of the strongest evidences for QGP formation [3]. The J/ψ is a bound state of the heavy "charmed" quark (c) and its antiquark ($\bar{c}$); the charmed quark mass m_c is about 1.5 GeV. Such quarks are not present in the colliding nucleons, and their creation in any thermal system is very unlikely due to their large mass. Therefore the only way c - $\bar{c}$ pair can be produced is by hard, pre-thermal scattering of the partons present in projectile and target at a very early stage of the collision. In a confining medium, they subsequently undergo soft hadronic interactions and bind to charmonium (J/ψ, ψ', ...). If a deconfining medium is produced, it will expand, cool off, and after the temperature drops to T_c, it will hadronize. When hadronization occurs, the c and the $\bar{c}$ are already far apart (in the deconfining medium no binding was possible). So they cannot find another heavy partner in the close neighborhood; instead they confine with u's and d's, which are present in large quantities, to form open charm (D mesons). Plasma formation thus

leads to enhanced open charm production, at the expense of the charmonium states.

Experimentally, one would like to compare the J/ψ signal in a process without deconfinement with one in which plasma formation was suspected.

The NA38 collaboration at CERN studied lepton pairs in the J/ψ mass region [36,43]. They measured the mass and the momentum of the muon pairs together with the associated (neutral) energy E_t for event characterization. In Fig.16, the muon pair spectra from ^{16}O-U collisions for $E_t<33$ GeV (peripheral) and $E_t>82$ GeV (central) are superimposed by matching the fitted Drell-Yan continua. At high E_t, the J/ψ signal has become considerably weaker; its decrease is shown by the shaded area. Any evidence for the ψ' has disappeared at high E_t. The results from ^{16}O-Cu and ^{32}S-U indicate a similar pattern. Since the projectile volumes are different, one needs a suitable variable for a direct comparison of the three cases. In Fig.17, the dependence of the J/ψ-to-continuum as function of $E_t/A^{2/3}$, which represents approximately the same transverse energy per unit volume in each case, is plotted. A common decrease of resonance-to-continuum ratio of about 50% between the lowest and the highest values of $E_t/A^{2/3}$ is observed. A careful study of the absolute cross-section of the continuum as function of $E_t$was carried out in order to show that indeed J/ψ suppression is present rather then a continuum enhancement [44]. Data on J/ψ suppression from p-U collisions, as measured by the NA38, do not show any significant E_t dependence. The observation of this suppression naturally led to an intensive theoretical consideration of alternative and more "conventional" suppression mechanisms. It now appears possible [45-47] to account for the measurements also by combining initial state gluon scattering with final state J/ψ absorption in very dense hadronic matter.

5.5 Direct Photons

Direct photons (real and virtual) and lepton pairs are considered to be the cleanest probes of quark-gluon deconfinement, since they interact weakly with the medium and escape from heated matter without being affected by final state interactions [53]. Thus, they offer the possibility of providing information about the temperature and the volume of the emitting source in its early, hottest stage. However, detection of direct photons is experimentally difficult due to the presence of a very high background from hadronic decays and from QCD hard photons. Up to now, only an upper limit, $\gamma/\pi^0<15\%$-20% has been reported [54].

5.6 Produced Particle Density Fluctuations (Intermittency)

For some time there has been evidence for the sporadic occurrence of large fluctuations in the (pseudo)rapidity distributions of hadrons in high energy collisions from both cosmics ray and accelerator experiments [49-50]. The fluctuations manifest themselves in single events as peaks, often called spikes, in narrow pseudo(rapidity) intervals. This phenomena was named intermittency. Studying such fluctuations may be interesting since large fluctuations are expected in the transition from quark-gluon plasma to hadron phase [7,52]. At CERN, a number of experiments have collected data on intermittency in heavy ion interactions (NA35,WA80, NA34, EUM01 ...). The results so far are inconclusive. A review of the experimental situation in this field can be found elsewhere in these proceedings [51].

6. CONCLUSIONS AND FINAL REMARKS

It seems that CERN experiments have reached the regime of very dense matter where quark-gluon plasma transition is expected. A considerable amount of nuclear stopping has been measured in ^{16}O and ^{32}S induced reactions. Observed transverse energy distribution extend to values of energy density of the order of 2-3 GeV/fm . The temperatures, derived from m_t spectra are of the same value for all produced particles and agree with the T_c (predicted critical value) for phase transition (~200 MeV).

Present experimental results show evidence for significant deviations from expected extrapolations of hadron-hadron reactions. Some of them, indeed, are consistent with expected QGP signatures (enhanced strangeness, suppressed J/ψ production, large freeze-out volume, perhaps intermittency).

However, alternative hadronic explanations are possible within models based on rescattering of the particles produced in the initial nucleon-nucleon collisions both among themselves and in the spectator nuclear matter.

There is NO CONCLUSIVE evidence of the QGP yet.

7. FUTURE

However, the experiments carried out so far are only a beginning. Further runs in 1991 and 1992 with ^{32}S beams will take place at the CERN SPS, and most of the experiments will be using improved equipment. For 1994 experiments with Pb beams of 170 GeV/N are planned. Thus, significant improvements in measurements of all relevant parameters can be expected, along with the possibility of observations of qualitatively new phenomena characteristic of large nuclear systems (~300 fm^3 for Pb beam) as opposed to

the present results, which may be more related to smaller systems such as p-p or p-nucleus.

The Relativistic Heavy Ion Collider (RHIC) which is presently under construction in BNL, is scheduled to come on line in 1997. It will accelerate countercirculating beams of heavy ions, all the way up to gold, to energies of 100 GeV/N (for protons the maximum beam energy will be 250 GeV). With this machine, the available range of rapidity will be extended to 10 units.

Furthermore, if LHC (Large Hadron Collider at CERN) is constructed, it will be able to collide heavy ions ot 4 TeV/N, which will extend the rapidity window even further, up to 20 units.

So, we are going to see a lot of interesting physics soon ...

Acknowledgement

It is with great pleasure that I take the opportunity to express my thanks to Professor John Cramer of the University of Washington in Seattle for reading the manuscript and for his helpful discussions and valuable suggestions.

FIGURES:

Fig.1 Multiplicity distribution in ^{32}S-Pb collisions at 200 GeV/N (NA36).

Fig.2 Transverse energy vs forward energy distribution in ^{32}S-Au collisions at 200 GeV/N (NA35).

Fig.3 Rapidity distribution of negative hadrons in ^{32}S-S collisions at 200 GeV/N (NA35).

Fig.4 Rapidity distribution of primordial protons in ^{32}S-S collisions at 200 GeV/N (NA35).

Fig.5 Transverse energy spectra for ^{16}O-Au at 60 and 200 GeV/N and ^{32}S-S at 200 GeV/N collisions (NA35).

Fig.6 Transverse mass distribution for ^{16}O-Au collisions at 200 GeV/N (NA35).

Fig.7 Transverse mass distribution for ^{32}S-S collisions at 200 GeV/N (NA35).

Fig.8 Freeze-out radii versus charged particle density at $y_{cms}=0$ for hadron-hadron and nucleus-nucleus collisions.

Fig.9 Ratio of the mean multiplicity $<\Lambda>$, $<\bar{\Lambda}>$, $<K^o>$ observed in NA35 acceptance to the negative hadron multiplicity $<h^->$ in ^{32}S-S collisions at 200 GeV/N.

Fig.10 Rapidity distribution for Λ's and $\bar{\Lambda}$'s in central ^{32}S-S collisions at 200 GeV/N (NA35).

Fig.11 Invariant mass plots for Λ's, $\bar{\Lambda}$'s and K^o's from ^{32}S-Pb collisions at 200 GeV/N (NA36).

Fig.12 Dimuon mass spectra in p-U, ^{16}O-U and ^{32}S-U collisions at 200 GeV/N (NA38).

Fig.13 $\Phi/(\omega+\rho)$ ratio as a function of transverse energy from ^{16}O-U and ^{32}S-U collisions at 200 GeV/N, normalized to the ratio measured in p-U events at 200 GeV/N (NA38).

Fig.14 $<p_t>$ as a function of dN/dy plots for Λ, $\bar{p}$, K^o, π from p-$\bar{p}$ collisions for particles with $p_t < 1.5$ GeV/c at $\sqrt{S}$ =1.8 TeV/N (Tevatron).

Fig.15 Distribution of multiplicity of photons from π^o decays in A-A collisions at 200 and 60 GeV/N (WA80).

Fig.16 The dilepton spectrum from ^{16}O-U collisions at low and high E_t, with matched continue. The shaded area indicated the observed J/ψ suppression (NA38).

Fig.17 The E_t dependence of J/ψ suppression in ^{16}O-Cu, ^{16}O-U and ^{32}S-U collisions. The dashed line indicates the overall J/ψ-to-continuum ratio in proton-uranium collisions (NA38).

REFERENCES:

1. e.g. J.B.Kogut, Nucl.Phys.**A418**,381c(1984).
   H.Satz, Nucl.Phys.**A418**,447c(1984).
   see also Proceedings of the Seventh International Conference on Ultra Relativistic Nucleus-Nucleus Collisions,
   Nucl.Phys.**A498**(1989),ed.G.Baym,P.Braun-Munzinger and S.Nagamiya.
2. R.Hagedorn and J.Rafelski, Phys.Lett.**97B**(1980)180.
3. T.Matsui and H.Satz, Phys.Lett.**B178**(1986)416.
4. L.D.McLerran and T.Toimela, Phys.Rev.**D31**(1985)545.
5. R.C.Hwa and K.Kajantie, Phys.Rev.**D32**(1985)1109.
   S.Raha and B.Sinha, Phys.Rev.Lett.**58**(1987)101.
6. M.Jacob and H.Satz, eds., Quark Matter Formation and Heavy Ion Collisions, proc. Bielefeld Workshop (May 1982), World Scientific, Singapore, 1982.
7. L.van Hove, Z.Phys.**C21**(1984)93.
   M.Gyulassy et al., Nucl.Phys.**B237**(1984)447.
8. C.Greiner in:"Hadronic Matter in Collisions 1988", World Scientific,1989,p.750, eds.P.Carruthers and J.Rafelski.
9. B.Bassalek et al., Z.Phys.**C38**(1988)45.
   T.Abbott et al., Phys.Lett.**B197**(1987)285.
10. H.von Gersdorf et al., Phys.Rev.**C39**(1989)1385.
11. A.Bamberger et al., Z.Phys.**C43**,25(1989).
12. S.Wenig, University of Frankfurt, Ph.D.Thesis(1990).
13. K.Werner, BNL Preprint, BNL-42435(1989).

14. H.Sorge et al., Ann.Phys.**192**(1989)266.
15. J.Schukraft et al., Nucl.Phys.**A498**(1989)79c.
16. J.W.Harris et al., Nucl.Phys.**A498**(1989)133c.
17. G.R.Young et al., Nucl.Phys.**A498**(1989)53c.
18. J.D.Bjorken, Phys.Rev.**D27**(1983)140.
19. R.Hagedorn, CERN 71-12(1971); GSI-Report 81-6(1981)236; Proceedings of Quark Matter 84, ed. K.Kajantie, Springer-Verlag(1985)53.
20. R.Hall et al., Proc.Workshop on Heavy Ion Physics at the AGS (HIPAG), Brookhaven, NY, USA,1990, report BNL-44911,p.16. M.Tannenbaum et al., Proc.Workshop on Heavy Ion Physics at the AGS (HIPAG), Brookhaven, NY, USA,1990, report BNL-44911,p.44.
21. R.Bamberger et al., Phys.Lett.**B203**(1988).
22. M.Lahanas and NA35 Coll., Quark Matter'90,Proc.8-th Int. Conf. on Ultrarelativistic Nucleus-Nucleus Collisions, Menton, France,1990. Nucl.Phys.**A525**(1991),p.327c.
23. P.Seyboth, ref 20,p.261.
24. R.Stock, Frankfurt preprint OKF 90-3 (1990).
25. K.Kajantie, Nucl.Phys. **A498**(1989)355c.
26. H.van Hecke and NA34 Coll., ref.22,p 227c.
27. R.Hanbury Brown and R.Q.Twiss, Nature **177**(1956)27 and Nature 178(1956)1046.
28. P.Koch, B.Muller, J.Rafelski, Phys.Rep.**142**(1986)167.
29. H.Eggers, J.Rafelski, Preprint AZPH-TH/90-28, submitted to J.Mod.Phys.
30. H.Strobele, proc. of this Workshop.
31. J.Harris et al., Nucl.Phys.**A498**(1989)133.
32. C. Gruhn et al., Joint International Lepton-Photon Symposium and Europhysics Conference on High Energy Physics, Geneva, July, 1991.
33. L.McLerran, Rev.Mod.Phys.58(1986)1021 and references therein. L.S.Schroeder, M.Gyulassy, Nucl.Phys.**A461**(1986).
34. B.Muller in: "Hadronic Matter in Collisions 1988", World Scientific,1989,p.739,eds.P.Carruthers and J.Rafelski.
35. J.Bartke et al., Univ. of Frankfurt Preprint (1990). M.Gazdzicki et al., Nucl.Phys.**A498**(1989)375c.
36. C.Baglin et al., Phys.Lett.**220B**(1989)
37. M.C.Abreu et al., Preprint LAPP-EXP-89-15(1989) contribution to the Europhysics Conference,Madrid,1989.
38. A.Shor, Phys.Rev.**54**(1985)1122.
39. P.Koch, U.Heinz and J.Pisut, Phys.Lett.**243B**(1990)149.
40. C.M.Ko and B.H.Sa, Preprint Texas A&M University,1990, submitted to Phys.Lett.B
41. L.van Hove, Z.Phys.**C27**,135(1985).
42. T.Alexopoulos et al., Phys.Rev.Lett.**64**,991(1990).

43. M.C.Abreu et al., (NA38) Z.Phys.C.-Particles and Fields**38**(1988)117.
L.Kluberg (NA38), Nucl.Phys.**A488**(1988)613c.
J.Y.Grossiord (NA38), Nucl.Phys.**A498**(1989)249c.
44. J.Varela, Nucl.Phys.**A525**(1991)275c.
45. S.Garin and M.Gyulassy, Phys.Lett.**214B**(1988)241.
46. J.Hufner,Y.Kurihara, H.J.Pirner, Phys,Lett.**215B**(1988)218.
47. J.Blaizot, J.Y.Ollitrault, Phys.Lett.**217B**(1989).
49. T.H.Burnett et al.(JACEE), Phys.Rev.Lett.**50**(1983)2062.
50. M.Adamus et al. (NA22), Phys.Lett.**B185**(1987)200.
51. Y.Takahashi, in this Workshop.
52. A.Bialas, R.Peschanski, Nucl.Phys.**B273**(1986)703-718.
53. P.V.Ruuskaanen, ref.22,p.255c.
L.D.McLerran and T.Toimela, Phys.Rev.**D31**(1989)545.
K.Kajantie and H.J.Miattinen, Z.Phys.C-Particles and Fields (1981)341.
E.V.Shuryak, Sov.J.Nucl.Phys.**28**(3)(1978)408.
54. T.Akesson et al., Z.Phys.C46(1990)369.
R.Albrecht et al, preprint CERN-PPE/91-01, submitted to
Z.Phys.C.(1991).
55. S.Abatzis et al., Phys.Lett.**B259**(1991)508.
J.L.Narjoux at al., ref.22,p.441c.

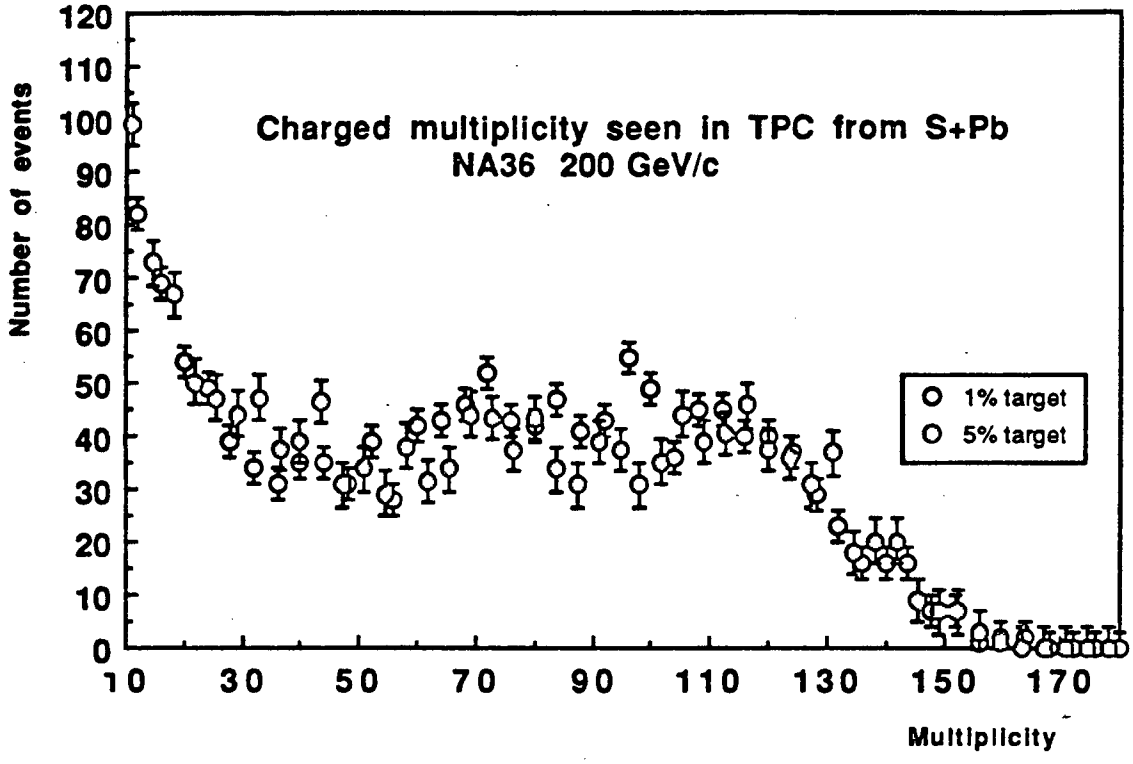

Fig.1 Multiplicity distribution in ^{32}S-Pb collisions at 200 GeV/N (NA36).

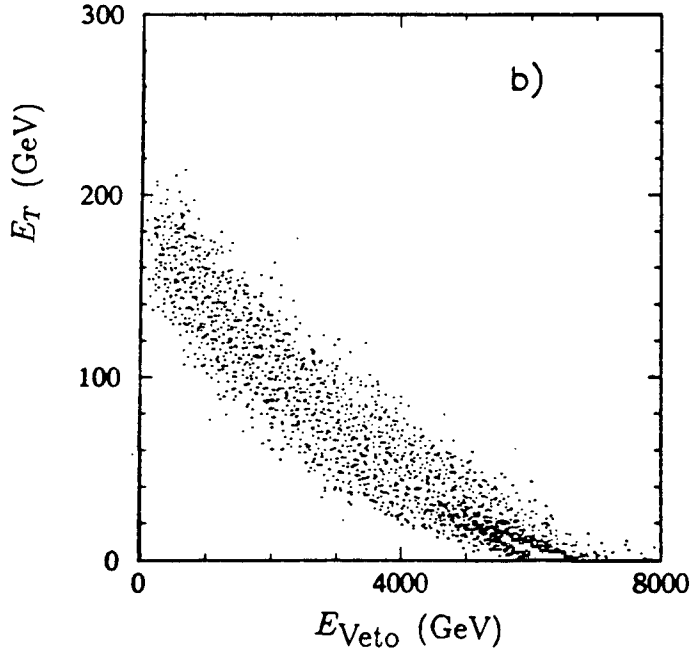

Fig.2 Transverse energy vs forward energy distribution in ^{32}S-Au collisions at 200 GeV/N (NA35).

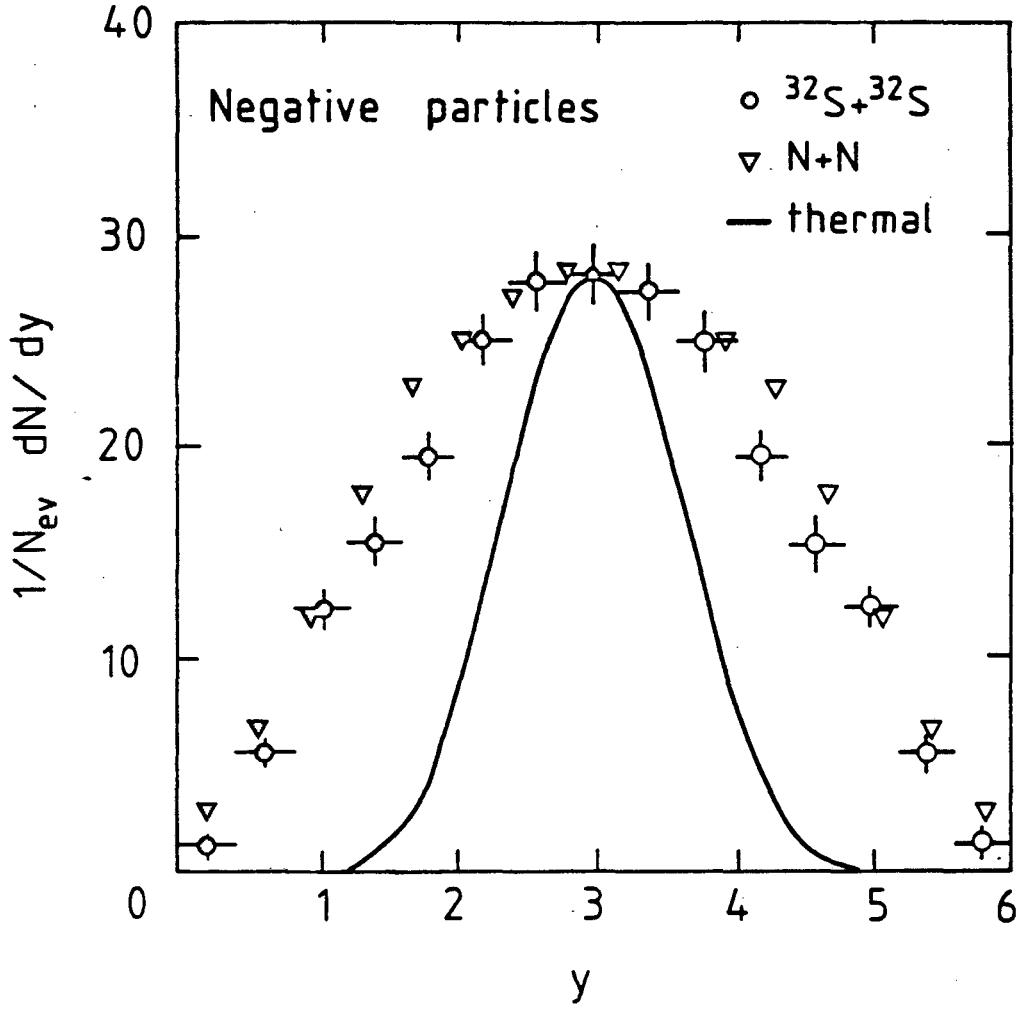

Fig.3 Rapidity distribution of negative hadrons in ^{32}S-S collisions at 200 GeV/N (NA35).

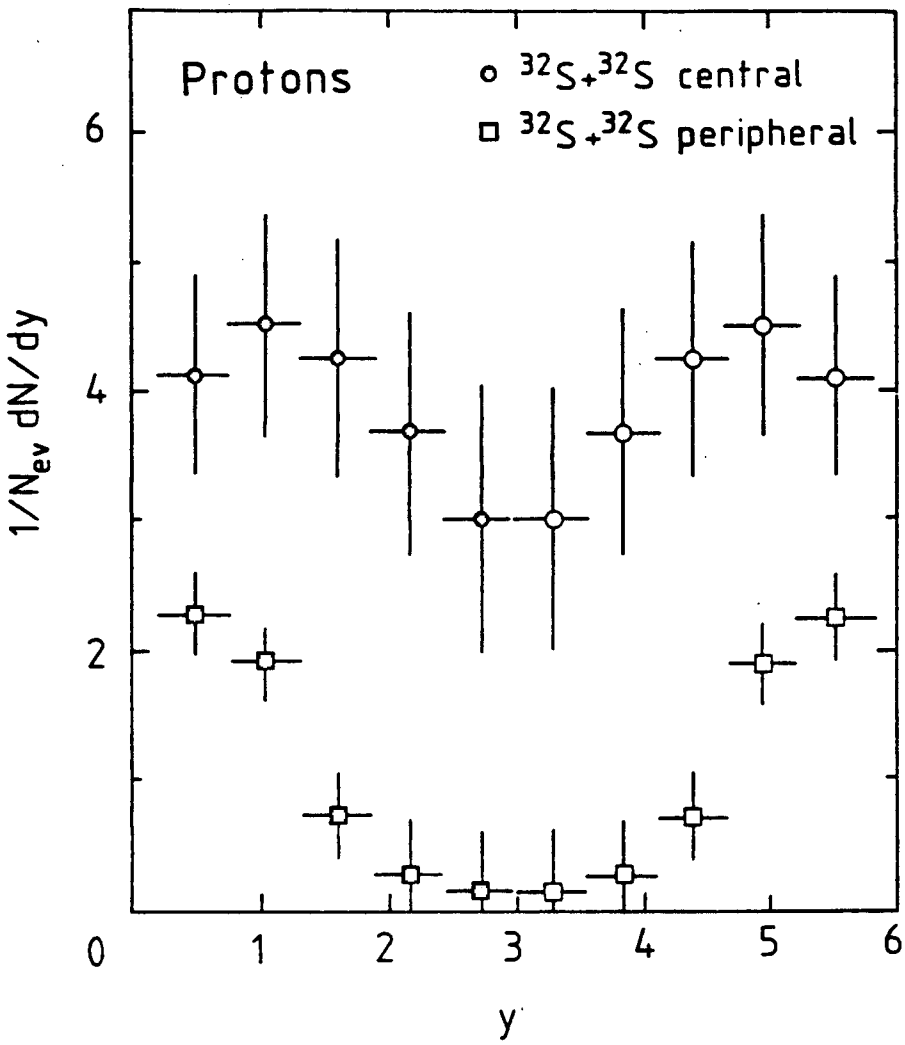

Fig.4 Rapidity distribution of primordial protons in ^{32}S-S collisions at 200 GeV/N (NA35).

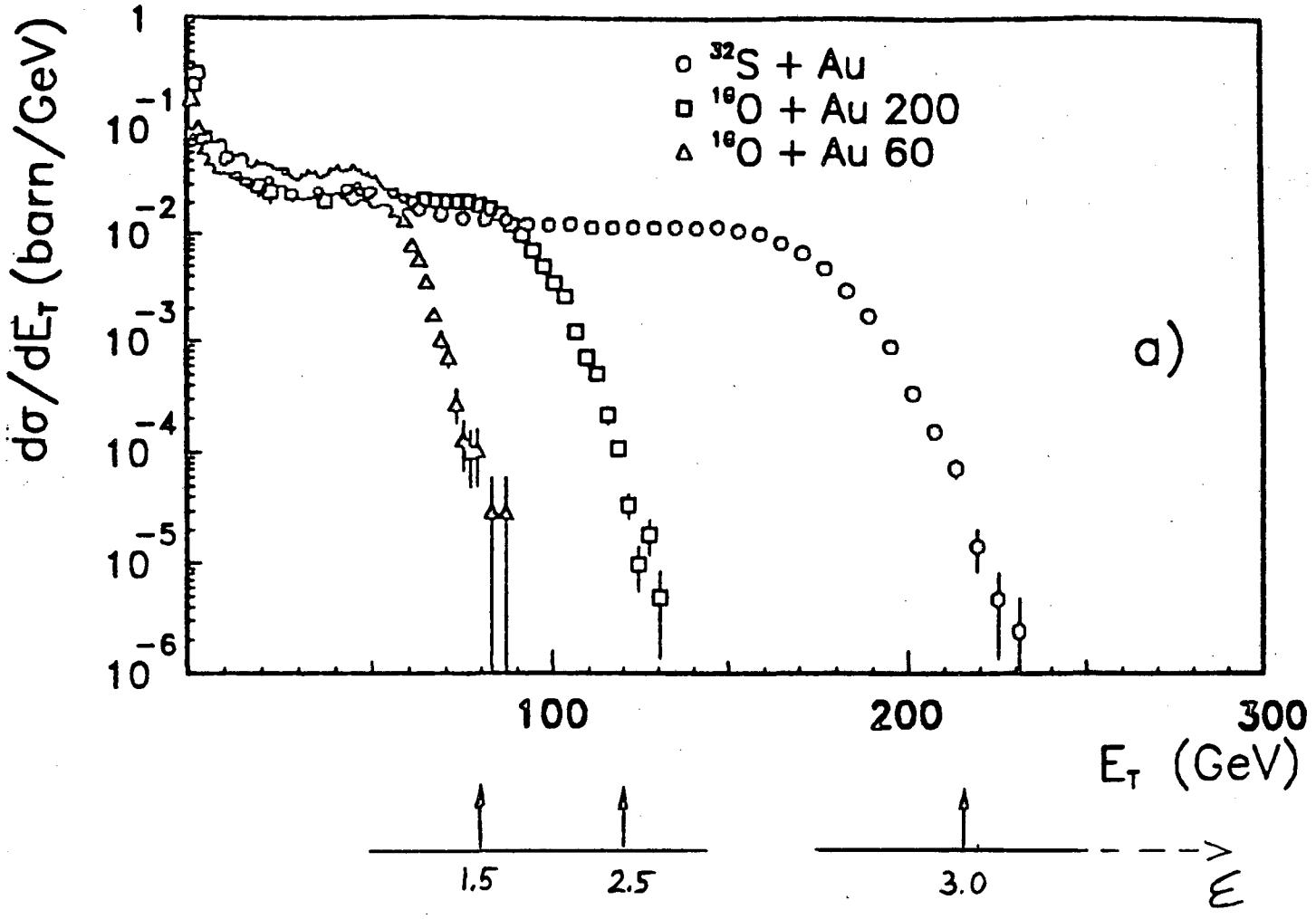

Fig.5 Transverse energy spectra for ^{16}O-Au at 60 and 200 GeV/N and ^{32}S-S at 200 GeV/N collisions (NA35).

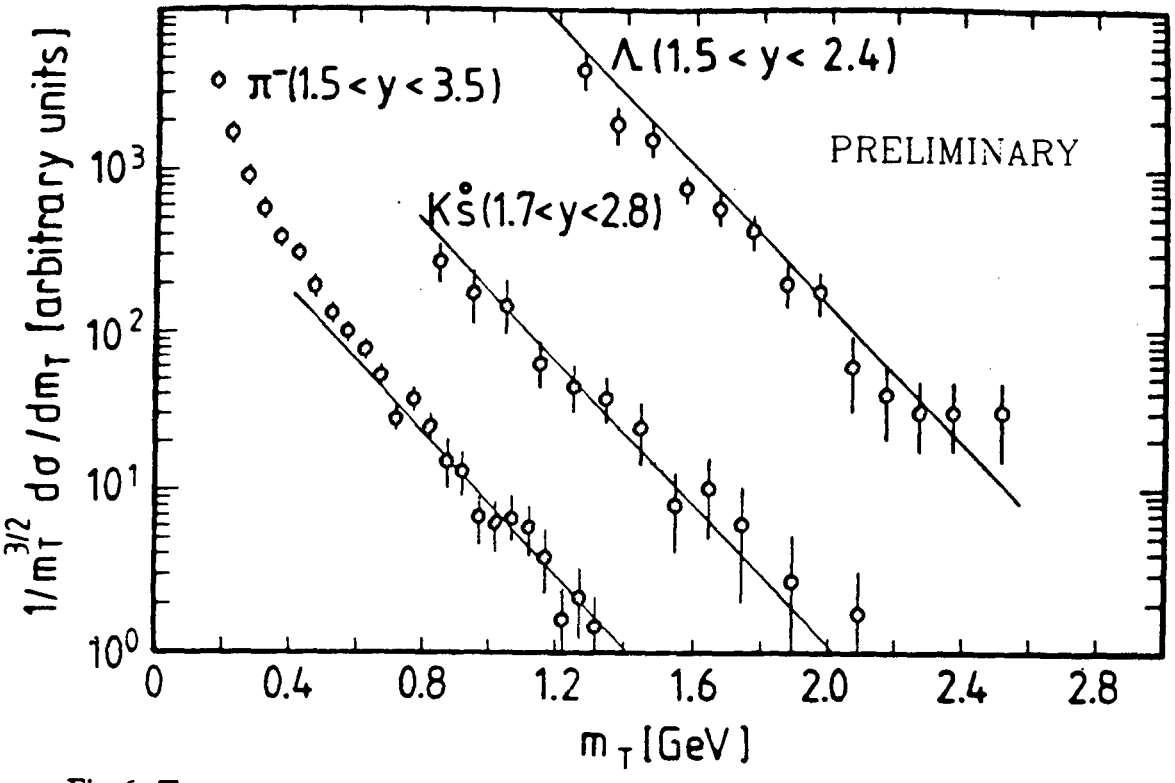

Fig.6 Transverse mass distribution for ^{16}O-Au collisions at 200 GeV/N (NA35).

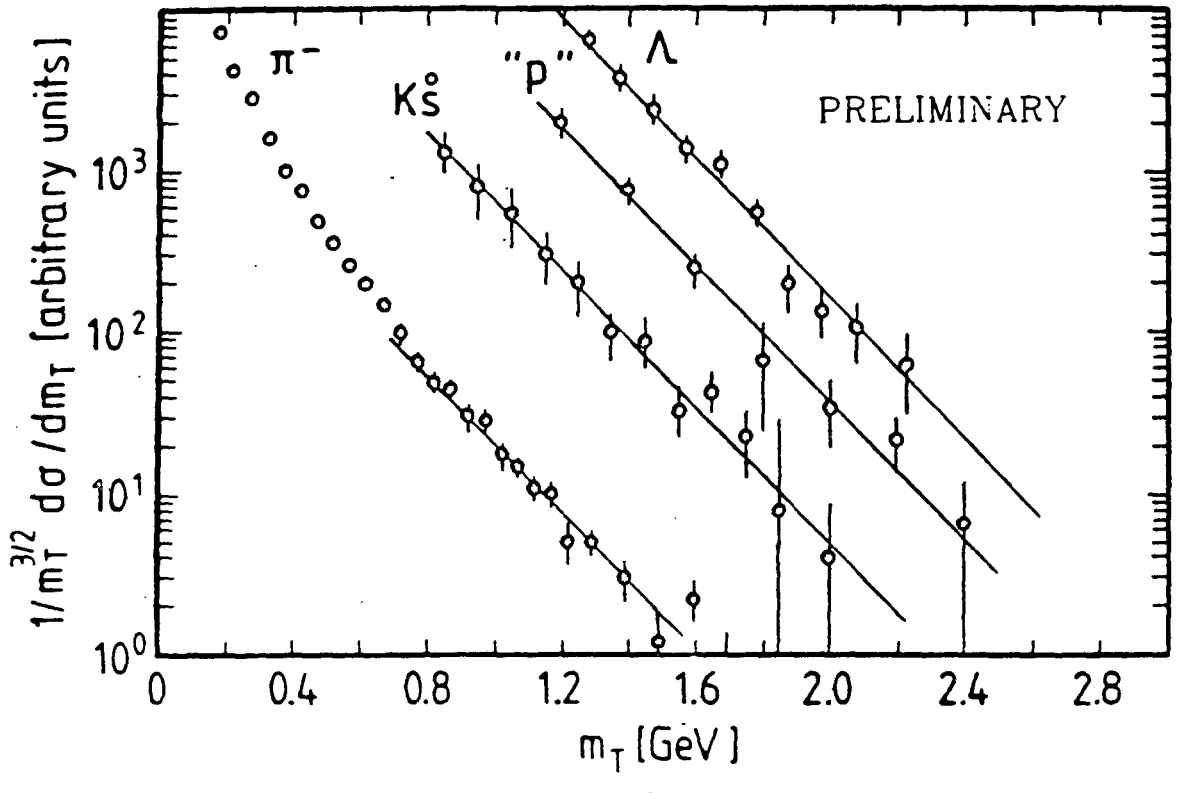

Fig.7 Transverse mass distribution for ^{32}S-S collisions at 200 GeV/N (NA35).

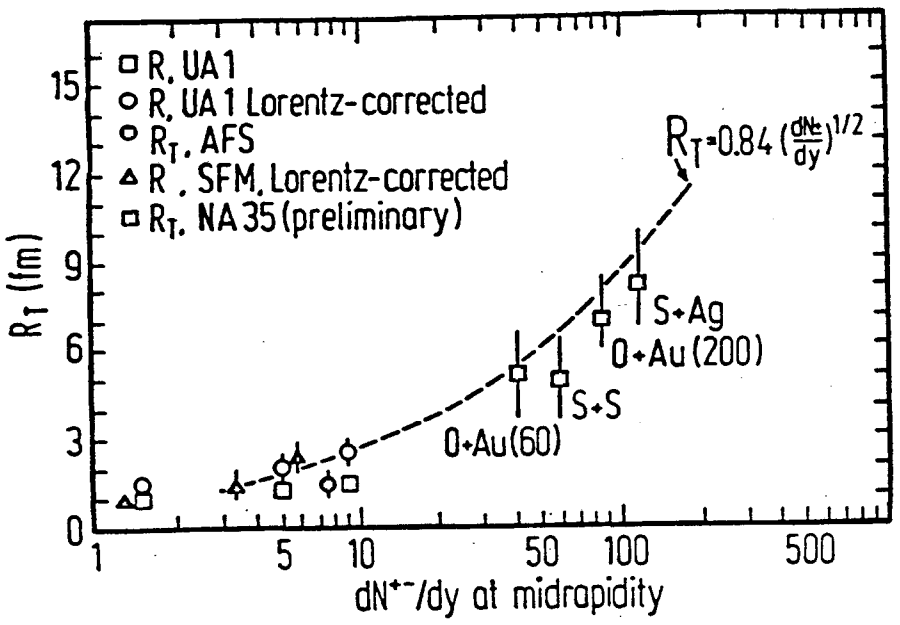

Fig.8 Freeze-out radii versus charged particle density at $y_{cms}=0$ for hadron-hadron and nucleus-nucleus collisions.

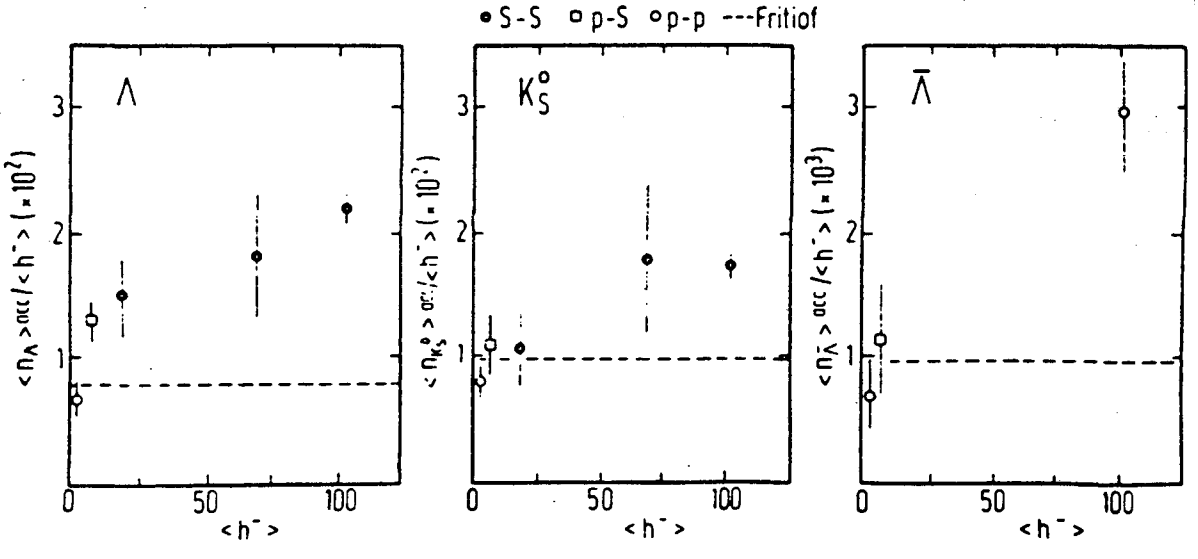

Fig.9 Ratio of the mean multiplicity <Λ>, < $\bar{\Lambda}$ >, <K^o> observed in NA35 acceptance to the negative hadron multiplicity <h^-> in ^{32}S-S collisions at 200 GeV/N.

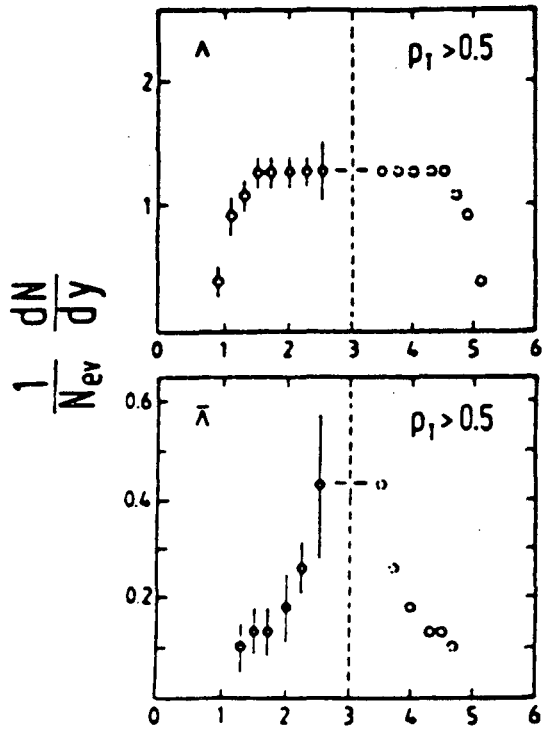

Fig.10 Rapidity distribution for Λ's and $\bar{\Lambda}$'s in central ^{32}S-S collisions at 200 GeV/N (NA35).

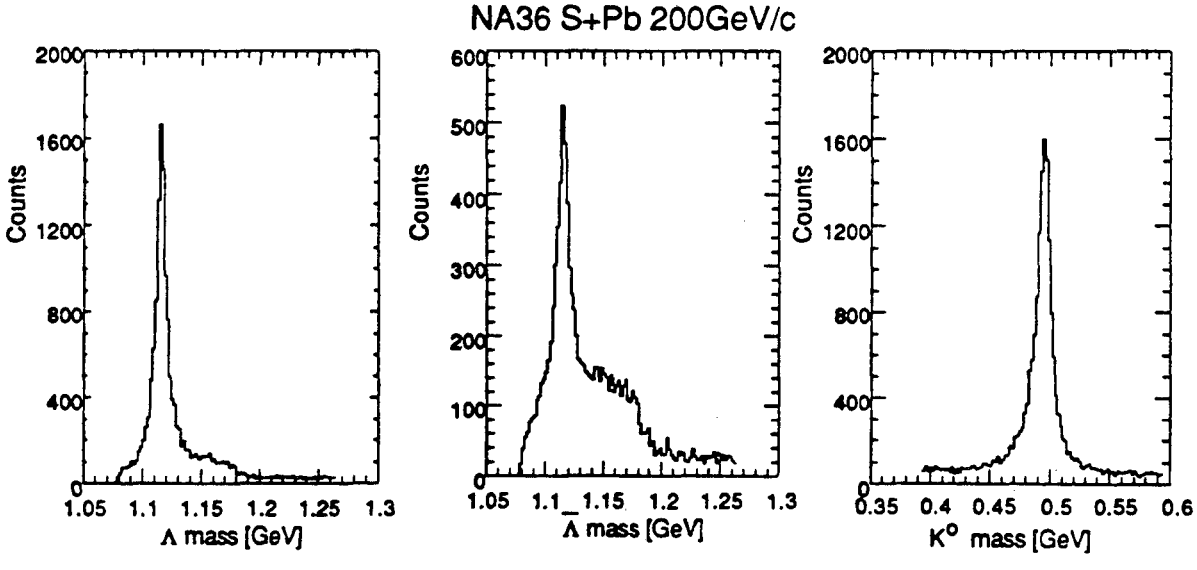

Fig.11 Invariant mass plots for Λ's, $\bar{\Lambda}$'s and K°'s from ^{32}S-Pb collisions at 200 GeV/N (NA36).

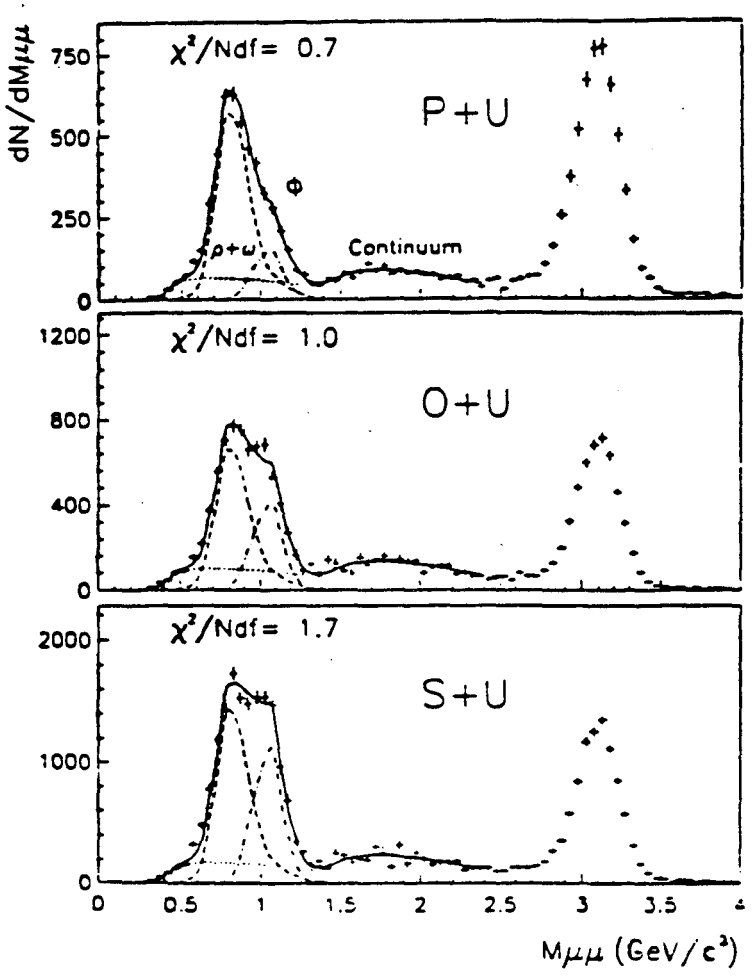

Fig.12 Dimuon mass spectra in p-U, ^{16}O-U and ^{32}S-U collisions at 200 GeV/N (NA38).

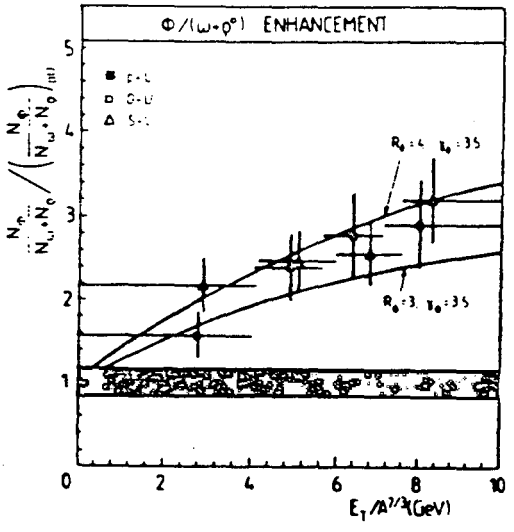

Fig.13 Φ/(ω+ρ) ratio as a function of transverse energy from ^{16}O-U and ^{32}S-U collisions at 200 GeV/N, normalized to the ratio measured in p-U events at 200 GeV/N (NA38).

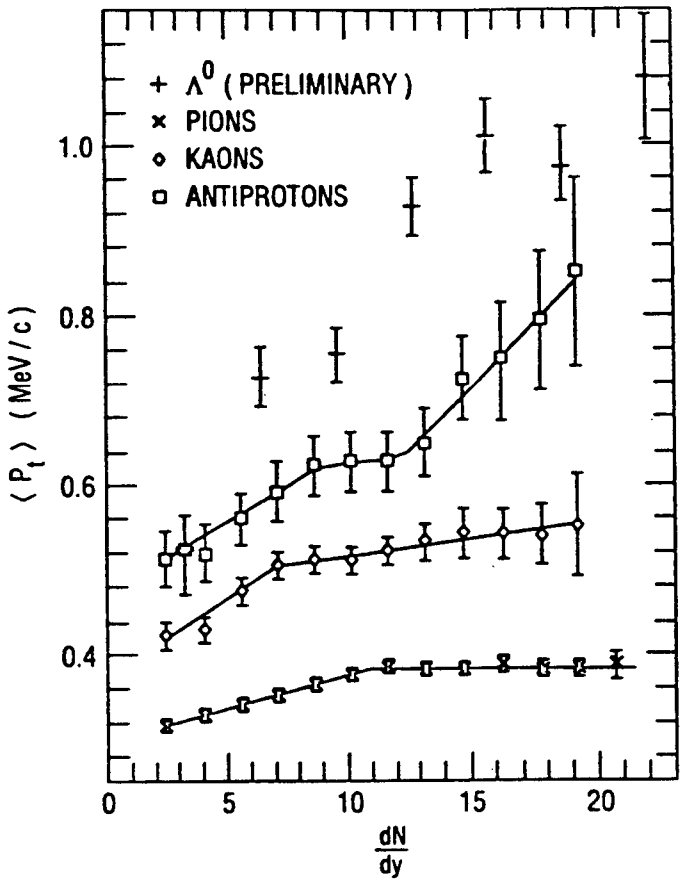

Fig.14 $\langle p_t \rangle$ as a function of dN/dy plots for Λ, $\bar{p}$, K^o, π from p-$\bar{p}$ collisions for particles with $p_t < 1.5$ GeV/c at $\sqrt{S}$ =1.8 TeV/N (Tevatron).

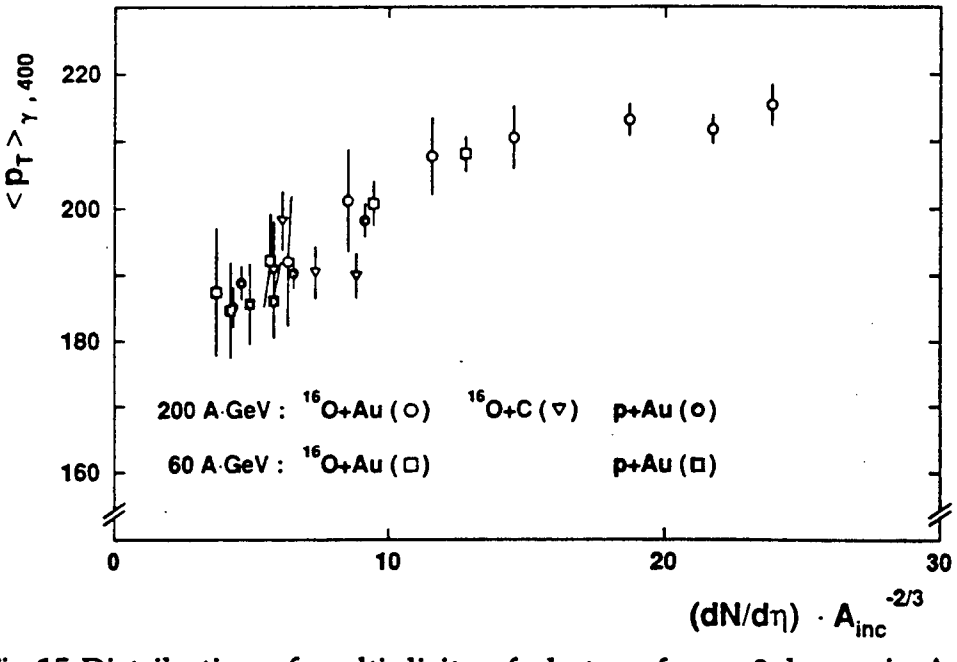

Fig.15 Distribution of multiplicity of photons from π^o decays in A-A collisions at 200 and 60 GeV/N (WA80).

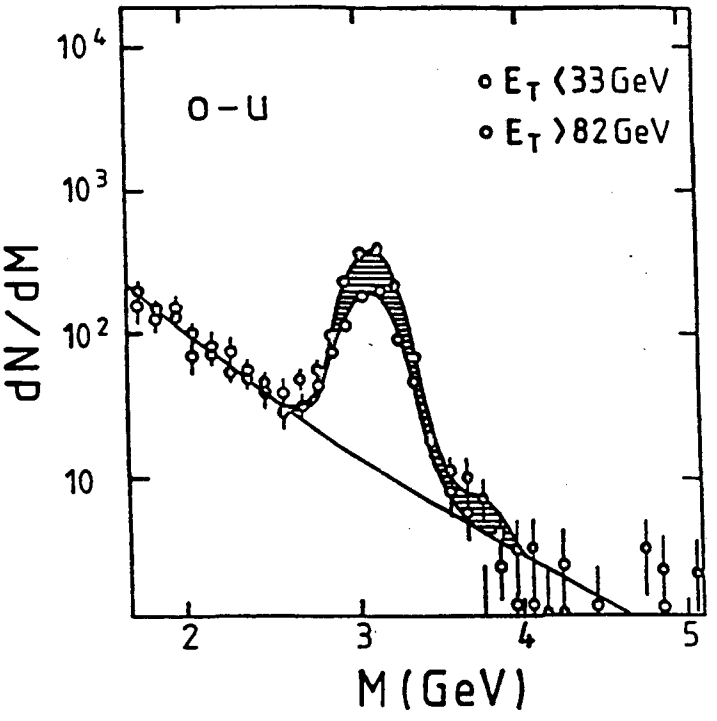

Fig.16 The dilepton spectrum from ^{16}O-U collisions at low and high E_t, with matched continue. The shaded area indicated the observed J/ψ suppression (NA38).

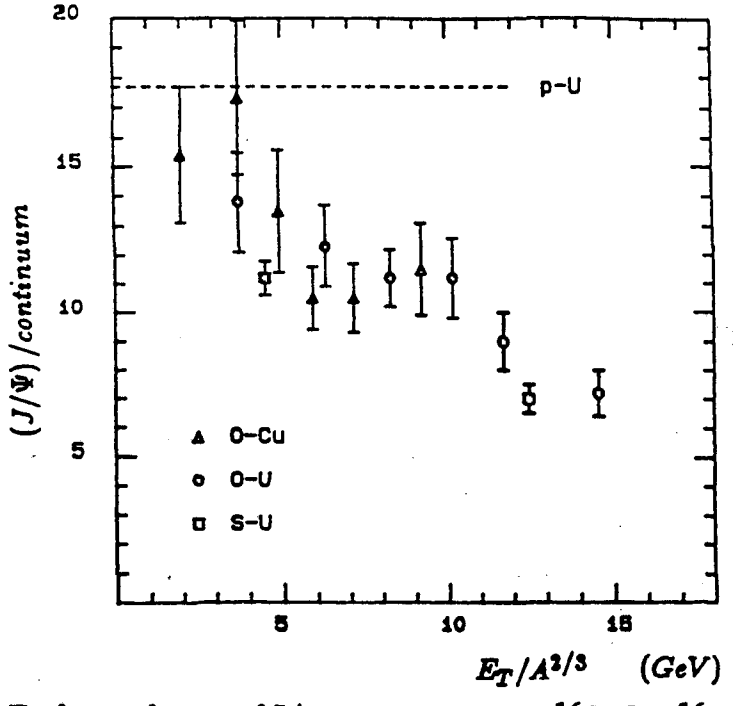

Fig.17 The E_t dependence of J/ψ suppression in ^{16}O-Cu, ^{16}O-U and ^{32}S-U collisions. The dashed line indicates the overall J/ψ-to-continuum ratio in proton-uranium collisions (NA38).

LAWRENCE BERKELEY LABORATORY
UNIVERSITY OF CALIFORNIA
INFORMATION RESOURCES DEPARTMENT
BERKELEY, CALIFORNIA 94720